Influence of carbonation on ionic transport in unsaturated concrete: evolution of porosity and prediction of service life

Mohamad Achour, Ouali Amiri, François Bignonnet, Emmanuel Rozière

Influence of carbonation on ionic transport in unsaturated concrete: evolution of porosity and prediction of service life

Mohamad Achour [a,b,c], Ouali Amiri[b,c], François Bignonnet[b,c] and Emmanuel Roziere[a,c]

[a] Ecole centrale de Nantes, Nantes, France
[b] Université de Nantes, Nantes, France
[c] GeM, Institute for Research in Civil and Mechanical Engineering, CNRS UMR 6183/FR 3473, France

ABSTRACT

In this paper, the effects of carbonation and moisture on chloride and ionic transport into concrete are studied. Based on the concrete composition and porosity as well as the physicochemical equilibrium, a comprehensive macroscopic model is proposed for this problem. The model features the chemical activity of ions, the interactions between chloride ions and concrete; and the ion–ion interactions in the solution. The governing equations of moisture and ionic transport into nonsaturated concrete are thoroughly described and solved numerically by the finite difference method in time and in space. Applications of the numerical model are demonstrated by predicting the evolution of the porosity and the service-life of a concrete specimen exposed to an aggressive environment containing chloride, carbon dioxide and moisture. A comparison of the model with a set of experimental data is finally proposed.

1. Introduction

The service life of a concrete structure is defined as the period of time during which the structure performs its function without repair. Service life depends on many variables; including environmental ones such as chloride, moisture and carbon dioxide penetration. Chloride ions from deicing salts or marine exposure penetrate into the concrete in solution in water. They may eventually reach the steel reinforcement, attack and break down the passivating layer and then accelerate the steel corrosion process.

The carbon dioxide contained in the air and moisture react with the cement hydration products: they both dissolve in the interstitial solution of the cementitious matrix of the concrete. This dissolution–precipitation process consumes hydroxyl ions, thus reduces the pH of the solution which may lead to the depassivation of steel reinforcement. This stage involves the transport of aggressive agents inducing the corrosion initiation (depassivation of reinforcement).

Although recent experimental observations and numerical analyses have shown the strong interaction between carbonation and chloride attack (Tumidajski & Chan, 1996), these phenomena have been separately studied in most of the existing researches on the corrosion of the concrete (Ababneh & Xi,2002; Leemann & Moro, 2017; Nguyen, 2008). Existing literature also shows that the effect of convection on the transport of chloride ions and carbon dioxide should not be neglected. The transport of moisture can accelerate the transport of ions (Phu Tho, 2014; Zhang, Wang, & Wittmann, 2014). Numerical models of the process of concrete corrosion damage take into account the microstructural

evolution (Ramezanianpour, Ghahari, & Esmaeili,2014). Recently a few studies have shown that for concrete subjected to both chloride ions ingress and carbonation, carbonation significantly influences the transport of chloride ions (Mai-Nhu, 2013; Wang, 2012). In the former study, the transport of chloride and carbon dioxide has been modelled without taking into account multi-ions transport especially HCO_3^- ions (Mai-Nhu, 2013). However, the concentration of CO_3^{2-} is a major parameter since it affects the passive layer of steel and modifies the transport properties of chloride ions (Liu et al., 2014). In the second work (Wang, 2012), the interaction between ions has been neglected, as well as the effect of microstructure evolution and the transformation of the hydration products. The present paper focuses on the initiation phase taking into account all these ions in the solution and the microstructural changes caused by carbonation through the evolution of porosity.

Some works proposed a direct modelling of the influence of carbonation on chloride transport in concrete (Lee & Yoon, 2003; Saeki, 2002). They consider chloride ions transport only due to diffusion and convection. The results show that the Friedel's salt ($3CaO.Al_2O_3.CaCl_2.10H_2O$) appears due to the chloride ions in the concrete. It will react after with carbon dioxide during the carbonation process. Finally, chloride ions are released to the pore solution in concrete, which can increase the free chloride concentration as follows:

$$4Ca^{2+} + 2Al(OH)_4^- + 2Cl^- + 4OH^- + 4H_2O \leftrightarrow 3CaO.Al_2O_3.CaCl_2.10H_2O \quad (1)$$

$$3CaO.Al_2O_3.CaCl_2.10H_2O + 3CO_2 \rightarrow 3CaCO_3 + Ca^{2+} + 2Cl^- + Al_2O_3 + 10H_2O \quad (2)$$

These two equations are characterised by the equilibrium constant $K_{FS} = 10^{-29.1}$ of precipitation of Friedel's salt (Nguyen, 2008) .The purpose of this study is to develop an original model able to describe the combined transport of chloride ions and carbon dioxide under various cycles of wetting and drying conditions. A multi-ions transport model has been built taking into account the physical interaction between ions and the chemical activity of all ions in the pore solution, in addition to the dissolution of CSH and portlandite and the precipitation of the calcite and silica gel. To our knowledge, the above mentioned parameters have never been taken into account in transport modelling.

The theoretical analysis of the model for this combined problem is given in Section 2. The numerical model, the input parameters, the boundary conditions and the solving method are presented in Section 3. The numerical results given in Section 4 are discussed on a concrete cover to predict its service-life. A comparison between experimental results and numerical results is proposed in Section 5.

List of Symbols

J_i flux of the ion i	D_i effective coefficient of diffusion of the ion i
Y_i coefficient of activity of the ion i	C_i concentration of the ion i
F Faraday constant	z_i valence of the ion i
R ideal gas constant	T temperature of concrete surface
V velocity of water	Ψ electrostatic potential
$C_{cl,b}$ concentration of bound chloride ions	$C_{i,f}$ concentration of free chloride ions
$\propto_L$ Langmuir constant	β_i Langmuir constant
T_{ref} reference temperature	D_i^{sat} coefficient of diffusion in saturated concrete
W water content	ε porosity of concrete
a_i activity of the ion i	r_i radius of ion i
e_0 charge of an electron	I ionic strength.
ϵ_0 electrical permittivity	K_H equilibrium constant of dissolving of CO_2
K_1 equilibrium constant of dissolving of H_2CO_3	K_2 equilibrium constant of dissolving of HCO_3^-
K_E equilibrium constant of autoprotolysis of water	K_β equilibrium constant of dissolving of $Ca(OH)_2$
K_c equilibrium constant of formation of $CaCO_3$	$S^0_{Ca(OH)_2}$ initial concentration and $Ca(OH)_2$
$\delta^0_{CaOH_2}$ kinetics of dissolving of $CaOH_2$	$S_{Ca(OH)_2}$ concentration of $Ca(OH)_2$
δ^0_{CSH} kinetics of dissolving of CSH	τ_{CSH} characteristic time of carbonation of CSH
R_0 radius of the crystal of $Ca(OH)_2$	$\bar{\gamma}_{CaOH_2}$ molar volume of $Ca(OH)_2$
$\Delta\epsilon$ evolution of the porosity of concrete	$\bar{\gamma}_{NaCl}$ molar volume of NaCl
C_{NaCl} concentration of NaCl	$\bar{\gamma}_i$ molar volume of $CaCO_3$
S_{CaCO_3} concentration of $CaCO_3$	S^0_{CSH} initial concentration of CSH
S_{CSH} concentration of CSH	$\Delta\bar{\gamma}_{CSH}$ variation of volume due to carbonation

List of Symbols

$\bar{\gamma}_{H_2O}$ molar volume of water	$\bar{\gamma}_i$ molar volume of ion i
C_{H_2O} concentration of water	K_e intrinsic permeability
S_e saturation degree	K_{re} relative permeability
P_c capillary pressure	μ_e viscosity of water
R_a resistance to air	D_{va} coefficient of diffusion of water vapor
ρ_e density of water	ρ_v density of water vapor
M_{H_2O} molar mass of water	$\varphi(W)$ water sorption-isotherms
ε_0 initial porosity	$D^0_{co_2}$ coefficient of diffusion of CO_2 in air
[i] concentration of ion i	$D_{CO_2/eff}$ effective coefficient of diffusion of CO_2
h and *D* are two constants which depends on the $Ca(OH)_2$ properties	

2. Theoretical study

2.1. Ionic transport

The transport of ions into concrete is a complex process. In order to study the effect of the interactions between all ions in the pore solution, in the model, this process is divided into four parts: (1) transport of ions by diffusion, (2) transport of ions by convection, (3) transport of ions due to the interactions between ions and (4) due to the chemical activity of the ions. The governing equation considering the flux J_i (mol m^{-2} s^{-1}) of ion specie *i* is given at the macroscopic scale by the extended Nernst Planck equation:

$$J_i = -D_i\left[\underbrace{\text{grad}C_i}_{\text{Diffusion}} + \frac{z_i F}{RT}\underbrace{C_i \text{grad}\psi}_{\text{Electrostatic}} + \underbrace{C_i \text{grad}}_{\text{Chemical activity}}\left(\ln Y_i\right)\right] + \underbrace{C_i V}_{\text{Convection}} \tag{3}$$

where D_i, C_i, z_i and Y_i are respectively, the effective coefficient of diffusion (m^2/s), the concentration (mol m^{-3}), the valence and the coefficient of activity of the ion *i*. *F* the Faraday constant (96,485,309 C mol^{-1}), *R* the ideal gas constant (83,143 J mol^{-1} K^{-1}), *T* the temperature (K), Ψ the electrostatic potential (V) and *V* the velocity of water (m/s).

2.2. Binding of chloride ions

A part of chloride ions are bound by the hydration products in the concrete, either through chemical binding or physical adsorption, while the other part is free in the pore solution, thus this can reach the reinforcing bars. A Langmuir isotherm is selected in this theoretical study to describe the equilibrium between free and bound chloride ions:

$$C_{cl,b} = \frac{\propto_L C_{cl,f}}{(1 + \beta_L C_{cl,f})} \tag{4}$$

where $C_{cl,b}$, $C_{cl,f}$, $\propto_L$ and β_L are respectively the concentration of bound and free chloride ions (mol m^{-3}), and the Langmuir constants. The latter will be adjusted to the values derived from experimental results.

2.3. Diffusivity of different ions

The model adopted by Buchwald (2000) is selected for the calculation of the effective coefficient of diffusion D_i for the ions in the pore solution. When the concrete is exposed to chloride and carbonation attack, D_i depends on the evolution of the porosity and on the saturation degree $S_e = \frac{W}{\epsilon}$. The equation is expressed as follows to calculate D_i:

$$D_i = D_i^{sat}\left(\frac{W}{\epsilon}\right)^{\lambda} \tag{5}$$

where D_i^{sat} is the coefficient of diffusion of ions in saturated concrete (m^2/s), which can be calculated from the coefficient of diffusion of ions in water, the tortuosity and the porosity of the concrete. W is the water content, ε is the porosity of concrete and λ is a parameter which can be calibrated with experimental results. In the literature $\lambda = 6$ is adopted (Nguyen, 2008; Wilke & Chang, 1955). The coefficient of diffusion of all ions in water is listed in the research works of Wilke and Chang (1955).

2.4. Electrostatic potential

Electrostatic interactions occur between the various ions present in the pore solution. These interactions can create an electrostatic potential Ψ which can be calculated from the extended Nernst Planck equation as follows in the case where the external electrical current $I_{ext} = F\sum_{i=1}^{n} z_i J_i$ is zero.

$$\text{grad}\Psi = \frac{-\sum_{i=1}^{n} z_i D_i W \text{grad}\left(C_{i,f}\right) - \sum_{i=1}^{n} z_i D_i W C_{i,f} \text{grad}\left(\ln Y_i\right) + \sum_{i=1}^{n} z_i C_{i,f} V}{\sum_{i=1}^{N} \frac{D_i z_i^2 F}{RT} W C_{i,f}} \tag{6}$$

The effect of the electrical double layer is not taken into account in our model so that the electro-neutrality condition imposes:

$$\sum_{i=1}^{n} z_i C_{i,f} = 0 \tag{7}$$

2.5. Chemical activity

Chemical activity accounts for the interaction between ions and the solution. The activity a_i of every ion can be calculated by:

$$a_i = Y_i C_{i,f} \tag{8}$$

With Y_i is the activity coefficient of ion i. In the literature many studies are aimed at determining the activity coefficient (Pankow, 1994). These studies are based on the Debye and Huckel (1923) model for a low concentration in the solution. The expression of Samson is used in our model (Samson, Marchand, & Beaudoin, 1999). The expression of the activity coefficient has been calibrated with experimental results for low and high concentrations in the solution. This expression is described as follows:

$$LnY_i = -A_{\emptyset} z_i^2 \left[\frac{\sqrt{I}}{1 + r_i b_{\emptyset}\sqrt{I}} + \frac{-\sqrt{I}\left(0.2 - 4.17 * 10^{-15} I\right)}{\sqrt{1000}}\right] \tag{9}$$

where $A_{\emptyset} = \frac{\sqrt{2}\, F^2 e_0}{8\pi (RT\epsilon_0)^{3/2}}$

$$b_{\emptyset} = \sqrt{\frac{2F^2}{RT\epsilon_0}}$$

$$I = 0.5\sum_{i=1}^{n} z_i^2 C_{i,f}$$

With r_i is the radius of ion i (m), e_0 is the charge of an electron (1.6×10^{-19} c), ϵ_0 is the electrical permittivity (8.85×10^{-12} F/m) and I is the ionic strength (mol/kg).

The value of the valence and the radius of ions present in the pore solution of the concrete are presented in the report of El Jouhari (2011).

Table 1. Chemical equilibrium for carbonation process.

$H_2O + CO_2 \leftrightarrow H_2CO_3$	$K_H = \frac{[H_2CO_3]}{[CO_2]}$	0.94
$H_2CO_3 + OH^- \leftrightarrow HCO_3^- + H_2O$	$K_1 = \frac{[HCO_3^-]}{[OH^-][H_2CO_3]}$	$10^{7.6}$ L/mol
$HCO_3^- + OH^- \leftrightarrow CO_3^{2-} + H_2O$	$K_2 = \frac{[CO_3^{2-}]}{[OH^-][HCO_3^-]}$	$10^{3.66}$ L/mol
$H_2O \leftrightarrow H^+ + OH^-$	$K_E = [OH^-][H^+]$	10^{-14} mol^2/L^2
$Ca(OH)_2 \leftrightarrow Ca^{2+} + 2OH^-$	$K_P = [OH^-]^2[Ca^{2+}]$	$10^{-5.19}$ mol^3/L^3
$Ca^{2+} + CO_3^{2-} \leftrightarrow CaCO_3$	$K_c = \frac{1}{[Ca^{2+}][CO_3^{2-}]}$	$10^{8.36}$ L^2/mol^2

2.6. Carbonation process

2.6.1. Physicochemical equilibrium

The carbonation process requires the presence of water because CO_2 dissolves in water forming H_2CO_3. During this process, $Ca(OH)_2$ and CSH dissolve to adjust the pH of the solution. $CaCO_3$ and silica gel are formed, which is likely to reduce the porosity of concrete. The governing equation of the carbonation process is expressed as follows:

$$Ca(OH)_2 + CO_2 \leftrightarrow CaCO_3 + H_2O \tag{10}$$

Table 1 gives the equilibrium corresponding to the two aspects of the carbonation process: dissolution of CO_2 and carbonation reaction (Thiery, 2005). K_H, K_1, K_2, K_E, K_P and K_c are equilibrium constants of the carbonation process.

For the rate of the carbonation reaction, the following equations are adopted by Thiery (2005) in order to calculate the concentration of hydration products and carbonation products:

$$\delta_{CaOH_2} = \frac{\partial S_{Ca(OH)_2}}{\partial t} = -X_P^0 \frac{1}{1 + \frac{h}{D}\frac{R_p(\gamma)}{R_c(\gamma)}\left(R_c(\gamma) - R_p(\gamma)\right)} \tag{11}$$

$$\delta_{CSH}^0 = \frac{\partial S_{CSH}}{\partial t} = -\epsilon S_e \frac{K_H}{\tau_{CSH}}[CO_2] \tag{12}$$

where $R_p(\gamma) = R_0(1-\gamma)^{1/3}$

$$R_c(\gamma) = R_0\left(1 - \gamma + \frac{\bar{\gamma}_{CaCO_3}}{\bar{\gamma}_{CaOH_2}}\gamma\right)^{1/3}$$

$$\gamma = 1 - \frac{S_{Ca(OH)_2}}{S^0_{Ca(OH)_2}}$$

$$X_P^0 = -h\, S_p(\gamma) \ln\left(\frac{[Ca^{2+}].[OH^-]}{K_p}\right)$$

$$S_p(\gamma) = \frac{3}{R_0}(1-\gamma)^{2/3} S^0_{Ca(OH)_2} \bar{\gamma}_{CaOH_2}$$

where δ_{CSH}^0 and $\delta_{CaOH_2}^0$ are the rate of dissolution of hydration products, $S^0_{Ca(OH)_2}$, $S_{Ca(OH)_2}$ are the initial and current concentrations of$Ca(OH)_2$, h and D are two constants that depend on the $Ca(OH)_2$ properties

(Thiery, 2005): h=5.6×10^{-4} mol m^{-2}.s^{-1}; D=1.5×10^{-14} mol m^{-1}.s^{-1}, R_0 is the radius of the crystal of $Ca(OH)_2$ = 3×10^{-5} m, τ_{CSH} is the characteristic time of carbonation of CSH (Thiery, 2005) (3000 s) and $\bar{\gamma}_{CaOH_2}$ and $\bar{\gamma}_{CaCO3}$ are the molar volumes of $Ca(OH)_2$ and $CaCO_3$ respectively.

2.6.2. Diffusivity of carbon dioxide

An empirical equation (13) is selected for the calculation of the effective coefficient of diffusion of CO_2 in the gas phase ($D_{CO_2/eff}$). This expression was first suggested by Papadakis, Vayenas, and Fardis (1991), and then calibrated against experimental data in Thiery's et al. research work (2003).

$$D_{CO_2/eff} = D^0_{co_2}\varepsilon^{2.74}(1-S)^{4.2} \tag{13}$$

where D^0_{co2} is the coefficient of diffusion of CO_2 in air at 25 °C, D^0_{co2} = 1.65× 10^{-5} m^2/s.

2.6.3. Evolution of the porosity due to ions transport and carbonation process

It is well known that the micro-structure of concrete is affected by ionic transport and carbonation process. In turn, the evolution of the microstructure impacts the transport properties of the concrete in a complex way. In the model, this impact is estimated through the evolution of the porosity in Equations (13) and (5). The evolution of the porosity can be estimated as follows (Thiery, 2005):

$$\Delta\varepsilon = \bar{\gamma}_{NaCl}C_{NaCl} + \bar{\gamma}_{CaCo_3}S_{CaCo_3} - \bar{\gamma}_{CaOH_2}\left(S^0_{CaOH_2} - S_{CaOH_2}\right) + \Delta\bar{\gamma}_{CSH}\left(S^0_{CSH} - S_{CSH}\right) \tag{14}$$

where $\bar{\gamma}_{NaCl}$, C_{NaCl}, S^0_{CSH}, S_{CSH} and $\Delta\bar{\gamma}_{CSH}$ are respectively the molar volume of NaCl and the concentration of NaCl, the initial and current concentrations of CSH calculated using eq. 12 and the variation of the volume due to carbonation of 1 mol of CSH. This equation is general and in this paper the decalcification process is not studied. In order to consider the porosity changes due to the chloride attack, the evolution of the volume changes of Friedel's salt (first part of the equation) is related to Equations (1) and (2). The second part of the equation describes the volume changes of hydration products during carbonation and precisely the formation of calcite and silica gel.

The volume balance of the pore solution can be calculated as follows (Marcus, 2005):

$$\sum_{i=1}^{n-1}\bar{\gamma}_i C_{i,f} + \bar{\gamma}_{H_2O}C_{H_2O} = 1 \tag{15}$$

with $\bar{\gamma}_i$ and $\bar{\gamma}_{H_2O}$ are respectively the molar volumes of the ions and of water. C_{H_2O} is the concentration of water. $\bar{\gamma}_i$ can be calculated by the following equation (Thiery, 2005):

$$\bar{\gamma}_i = \frac{4}{3}\pi r_i^3 N_A - 4.2\frac{z_i^2}{r_i} \tag{16}$$

with N_A is the Avogadro's number = 6.022× 10^{23}.

2.7. Moisture transport

The model adopted for the moisture transport takes into account the water released by the carbonation process Equation (10). This equation can be derived as follows:

$$\frac{\partial S_e}{\partial t} = -\frac{K_e K_{re}}{\epsilon\mu_e}\frac{\partial P_c}{\partial S_e}\text{grad}S_e + \frac{R_a D_{va}}{\rho_e}\frac{\partial \rho_v}{\partial S_e}\text{grad}S_e - \frac{M_{H_2O}}{\rho_e}\frac{\partial S_{CaOH_2}}{\partial t} \tag{17}$$

where μ_e, ρ_e and M_{H_2O} are respectively the viscosity, the density and the molar mass of water. ρ_v is the density of water vapor and S_e is the saturation degree of concrete.

(A) The coefficient of diffusion of water vapor

$D_{Va} = 2.75 \times 10^{-5}\left(\frac{T}{T_{ref}}\right)^{1.88}$ is the coefficient of diffusion of water vapor (m^2/s) and T_{ref} is the reference temperature = 20 °C.

(B) The capillary pressure

$P_c = -\rho_e \frac{RT}{M_{H2O}} \ln\varphi(W)$ is the capillary pressure (atm) calculated from $\phi(W)$, which describes sorption and desorption isotherms (see next Section Equation (19)). These isotherms can be derived from experimental results depending on the type of concrete and on wetting-drying cycles (Phu Tho, 2014).

(C) Intrinsic permeability

$K_e(m^2) = K_e^0\left(\frac{\varepsilon}{\varepsilon_0}\right)^2\left(\frac{1-\varepsilon_0}{1-\varepsilon}\right)^2$ depends on the initial porosity of concrete ε_0. This permeability is obtained from van Genuchten's study (1980).

(D) Relative permeability

$K_{re}(m^2) = (S_e)^{0.5}\left[1-(1-(S_e)^{1/0.34})^{0.34}\right]^2$ (Mualem, 1976).

(E) Resistance to the air

$R_a = (\varepsilon)^{2.74}(1-S_e)^{4.8}$ (Thiery's work (2005) based on Millington's study (1959)).

3. Numerical model and boundary conditions

The discretisation approach for a 1D domain adopted in this study has also been employed by Mai-Nhu (2013) and Nguyen and Amiri (2016) to model the ionic transport and carbonation process of concrete. The presented numerical results have been carried out by dividing a 75 mm concrete specimen into 75 nodes and using a time step of 1 h. The boundary conditions correspond to a concrete specimen covered with aluminium on all sides except the surface exposed to air and aggressive solution. The flow chart on how different equations of Section 2 are linked is presented in Figure 1 for the coupled transport of chloride ions and carbonation under different wetting–drying cycles.

The concrete mixture used in this study has been designed and characterised by Khokhar et al. (2010) and Nguyen and Amiri (2016) as shown in Table 2. This concrete is selected from the literature because the input data and the parameters needed in the model are available. The composition of the concrete is given in Phu Tho's work (2014). The concrete has a density of 2340 kg/m^3. The water porosity was measured by water porosity test ($\epsilon_0 = 15\%$) and the concrete had an initial water permeability of 10^{-20} m^2. As the experimental determination of this parameter is difficult, it was estimated from Baroghel-bouny's research work (1994).

The concrete specimen is initially partially saturated ($S_e^0 = 70\%$) and then exposed to combined carbonation (0.02 mol/L) and chloride attack (0.5 mol/L) under 6 h/6 h of wetting and drying cycles ($S_e^{t>0} = 92\%$ wetting, $S_e^{t>0} = 60\%$ drying).

The governing equation considering the diffusivity, ions interactions, ions activities and convective terms is given by:

$$\frac{\partial\left(WC_{i,f}\right)}{\partial t} + (1-\varepsilon)\frac{\partial C_{i,b}}{\partial C_{i,f}}\frac{\partial C_{i,f}}{\partial t} + \mathrm{div}\left(-D_i\left[W\,\mathrm{grad}C_{i,f} + \frac{Wz_iF}{RT}C_{i,f}\,\mathrm{grad}\Psi + WC_{i,f}\,\mathrm{grad}\left(\ln Y_i\right)\right] + WC_{i,f}V\right) = 0 \tag{18}$$

In this study only the interaction between chloride ions and concrete has been considered so: $C_{i,b} = 0$ if $i \neq Cl^-$.

For carbonation and moisture transport we consider Equations (11), (12) and (17). These equations are solved using a dedicated programme-based on finite difference discretisation with an implicit scheme (Despres,2014; LeVeque, 1998). The input data used to describe the binding isotherm of chloride

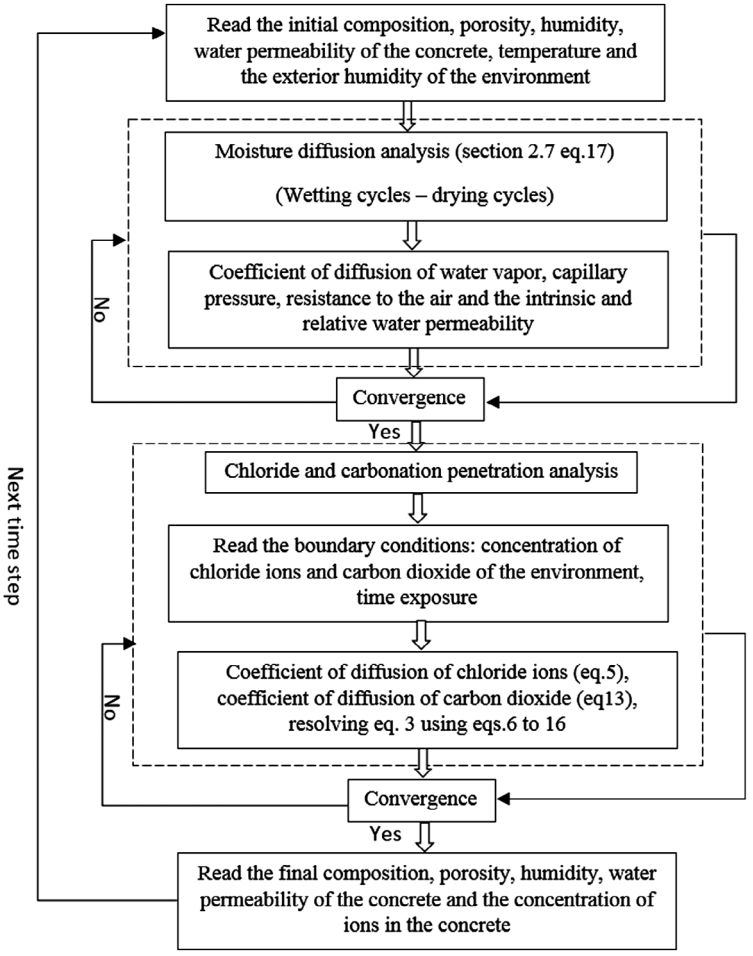

Figure 1. Flowchart of the numerical model.

Table 2. Composition of the concrete specimen.

Materials used Khokhar et al. (2010) and Nguyen and Amiri (2016)	Value
Gravel 10/14 mm	836 kg/m^3
Gravel 6/10 mm	201 kg/m^3
Sand 0/4 mm	816 kg/m^3
Cement CEM I 52.5 N	103 kg/m^3
Blast furnace slag	310 kg/m^3
Water	170 kg/m^3
Superplasticiser	1.89 kg/m^3
Effective water/Binder	0.41

ions, and the water sorption–desorption isotherms are determined in Phu Tho's research work (2014) as follows:

(A) Sorption/desorption isotherms

To investigate water vapour sorption and desorption of concrete specimen, the BELSORP-aqua3 is used to measure water vapour isotherms (Bel Japan catalog, 2010; Xi, Bažant, & Jennings, 1994). The expression of these isotherms in each case (sorption-desorption) generated by the instrument is as follows:

Table 3. Input data for the numerical model.

Input Data	Method of calculation	Measured value
Porosity	Water porosity (Phu Tho 2014)	0.15
Density of concrete	Experimental calculation (Phu Tho 2014)	2340 kg/m^3
Sorption/desorption isotherms	BELSORP-aqua3 (Phu Tho 2014)	Sorption $W = \frac{94.64\varphi}{1+5915\varphi}\frac{1-0.121\varphi}{1-0.935\varphi}$ Desorption $W = \frac{26.706\varphi}{1+445.1\varphi}\frac{1-0.637\varphi}{1-0.902\varphi}$
Coefficient of diffusion of chloride ions	Migration test (Phu Tho 2014)	0.54×10^{-12} m^2/s
Binding isotherms between chloride and hydration products	GranDuBé (Phu Tho 2014)	Langmuir isotherm $C_{cl,b}(\text{mol/m}^3) = \frac{0.00013C_{cl,f}}{1+0.0004C_{cl},f}$
Water Permeability	Literature Baroghel-Bouny's (1994)	1×10^{-20} m^2

Table 4. Molar volumes used in the model from Thiery (2005).

$\bar{V}_{CaOH_2}$	33×10^{-6} m^3/mol
$\bar{V}_{CaCO_3}$	35×10^{-6} m^3/mol
$\bar{V}_{CSH}$	86×10^{-6} m^3/mol
$\bar{V}_{\text{Friedel's salt}}$	272×10^{-6} m^3/mol
$\bar{V}_{H_2O}$	18×10^{-6} m^3/mol
$\Delta\bar{V}_{CSH}$	2.3×10^{-6} m^3/mol

Table 5. Initial and boundary conditions for the coupled transport problem. (carbonation and chloride attack).

Initial conditions	Boundary conditions
$[CO_2]\,(x, t = 0) = 0$	$[CO_2]\,(x = 0, t > 0) = 0.02$ mol/L
$[Cl^-]\,(x, t = 0) = 0$	$[Cl^-]\,(x = 0, t > 0) = 500$ mol/m^3
$S_{CSH}(x, t = 0) = 3.1$ mol/L	6 h/6 h of wetting and drying cycle
$S_{C3A}(x, t = 0) = 0.025$ mol/L	$S_e(x = 0, t > 0) = 92\%$ wetting
$S_{Ca(OH)_2}(x, t = 0) = 2.35$ mol/L	$S_e(x = 0, t > 0) = 60\%$ drying
$S_e(x, t = 0) = 70\%$	$[Na^+]\,(x = 0, t > 0) = 500$ mol/m^3

$$\text{Sorption} \quad W = \frac{94.64\varphi}{1+5915\varphi}\frac{1-0.121\varphi}{1-0.935\varphi}$$

$$\text{Desorption} \quad W = \frac{26.706\varphi}{1+445.1\varphi}\frac{1-0.637\varphi}{1-0.902\varphi} \tag{19}$$

(B) *Binding isotherms between chloride and hydration products*

In order to take into consideration the interaction between chloride ions and the hydration products of the concrete, binding isotherms were measured on different concrete specimens (Phu Tho, 2014) according to GranDuBé procedure (Amiri & Aït-mokhtar, 2007). The results show that a Langmuir isotherm can be used to link free and bound chlorides:

$$C_{cl,b}\left(\text{mol/m}^3\right) = \frac{0.00013C_{cl,f}}{1+0.0004C_{cl},f} \tag{20}$$

The summary of all input data used in this paper is presented in Tables 3 and 4.

4. Results and discussion

The flowchart described in Figure 1 has been applied to solve the combined transport problem on the concrete chosen in Section 3 with the initial and boundary conditions listed in Table 5. This numerical resolution determines the concentration of all output data, namely the concentration of all ions in the solution, the solid fraction, the porosity and the saturation degree of the concrete.

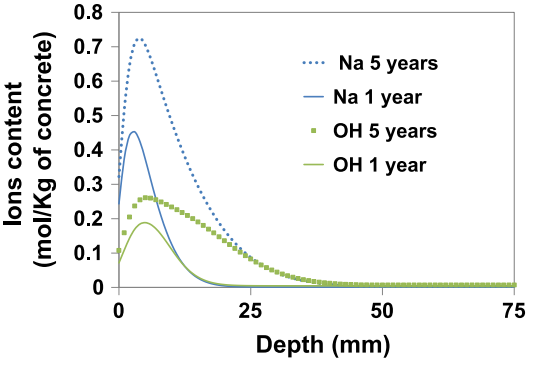

Figure 2. Depth profile of some alkaline ions after 1 and 5 years of exposure.

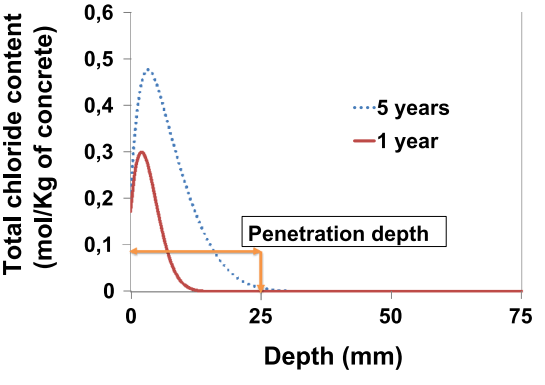

Figure 3. Profiles of chloride content after 1 and 5 years of exposure, and chloride penetration depth after 5 years.

4.1. Ions transport in concrete under cyclic drying–wetting conditions

As presented before, several ions are taken into account in our model for the concrete specimen. The concentration of some of these ions is difficult to identify experimentally. Figures 2 and 3 show the profiles of sodium, hydroxyl and chloride ions after an exposure period of 1 and 5 years, respectively, with 6 h/6 h of wetting and drying conditions.

When concrete is subjected to a drying–wetting environment, the transport of ions and particularly chloride ions into concrete cannot be ignored. When concrete is exposed to one year of aggressive environment, the concentration of chloride ions at 5 mm is significant. Figure 4 illustrates the sensitivity of the model to the rate of drying–wetting cycles, which is experimentally known to influence the ionic transport (Wang & Lu, 2007). It is due to the alternative drying and wetting, which affect the pore solution equilibrium so that chloride transport is accelerated and the transport of alkaline ions is also affected mainly near the surface of the concrete.

The effect of convection on the chloride penetration into concrete can be studied. Figure 5 compares the penetration by diffusion only or by combined diffusion and convection as computed from the model. It is clear that the effect of convection on chloride penetration is significant.

4.2. Change in micro-structure due to carbonation and its effect on chloride ions penetration

The penetration of chloride ions in concrete depends on the micro-structure. During chloride attack, Friedel's salt crystallises as per Equation (1). During carbonation, CO_2 reacts with Friedel's salt and

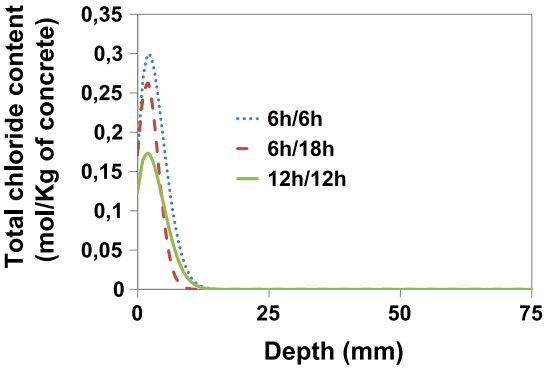

Figure 4. Profile of chloride ions for different rates of drying–wetting cycles during 1 year of exposure.

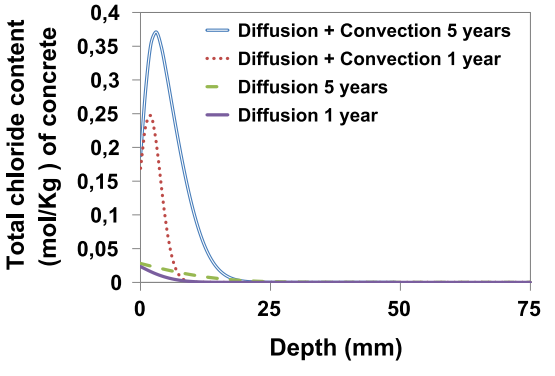

Figure 5. Effect of convection on free chlorides profiles after 1 and 5 years of test period.

frees chloride ions from hydration products as per Equation (2). These two equations determine the amount of Friedel's salt using the chemical equilibrium. Therefore, the concentration of chloride ions increases in the pore solution. Figure 6 illustrates the consumption of Friedel's salt due to these combined phenomena.

The reaction of carbonate ions with calcium ions released by $Ca(OH)_2$ and CSH result in a drop of pH. These hydration products actually dissolve to adjust the pH of the solution. In addition, new products as silica gel and $CaCO_3$ precipitate on $Ca(OH)_2$ and on CSH. The formation of these products induces a decrease in the porosity of concrete via Equation (14). Figure 7 shows the distribution of all solid components in the concrete. Our model allows the prediction of the contents of all solid phases in the concrete through time. The results shown in Figure 7 are obtained for 1 year of test period.

The concrete composition is significantly modified in the first 2 cm (Morandeau, 2013; Phu Tho, 2014; Villain & Thiery, 2006). The pore volume of carbonated concrete has dropped from 15% to around 13% after 1 year of exposure. The $CaCO_3$ content is an index of the degree of carbonation, just as the amount of $Ca(OH)_2$ and CSH describe the degree of hydration. The following section deals with the service life of concrete exposed to chloride, moisture and carbon dioxide from the environment for many years so as to assess the thickness of concrete cover to ensure concrete durability.

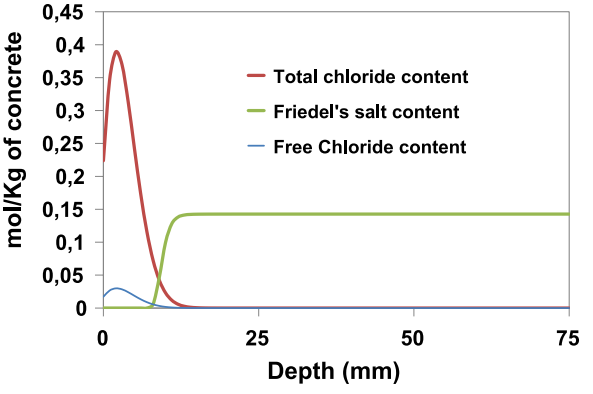

Figure 6. Consumption of Friedel's salt due to carbonation after 1 year of test period.

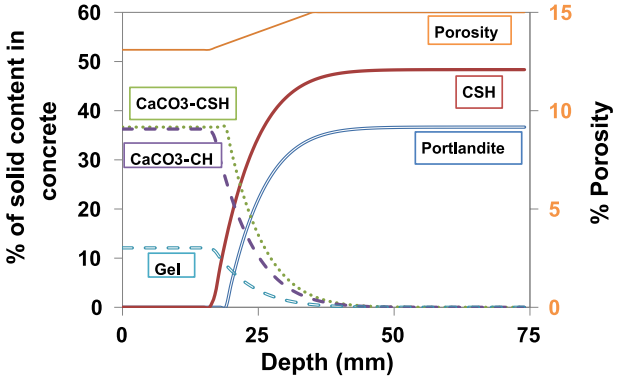

Figure 7. Amount of solid components after 1 year of test period.

4.3. Prediction of the service life of reinforced concrete exposed to chloride, wetting/drying and carbon dioxide from the environment

A service life of at least 50 years is required for most of structures. Many options are provided to the designer, among which a range of concrete cover depths adapted to the exposure to chloride ions and carbon dioxide. In this section, a case study representing a more realistic problem *in situ* is performed. We will describe the influence of carbonation on the penetration of chloride ions. The concrete specimen is exposed to wetting drying cycles for 10, 20 and 50 years.

Figure 8 shows two cases of chloride penetration depth. This penetration depth is defined as the distance from concrete surface till the depth where the concentration of chloride ions is negligible (see Figure 2 for the 5 years case). Case 1 describes the penetration depth of chloride ions taking into account both carbonation process and chloride ions transport, while case 2 takes into account chloride ions transport only.

As we can see from Figure 8 the penetration depth of chloride ions is higher for case 1 (Mai-Nhu, 2013; Wang, 2012). Thus, the effect of carbonation on the chloride attack and service life analysis should be considered when designing reinforced concrete structures, in order to estimate more precisely the concrete cover depth appropriate for the expected service life. Saillio (2013) has experimentally shown that carbonation decreases the chloride binding capacity of concrete so that the chloride ingress is accelerated.

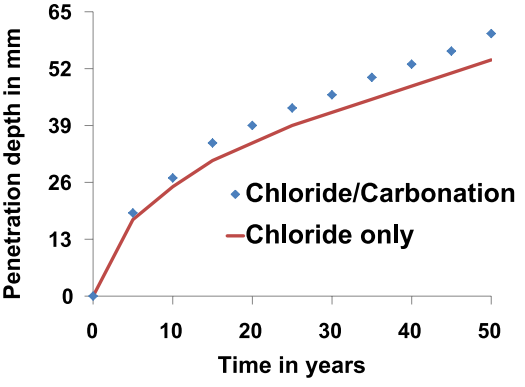

Figure 8. Chloride penetration depth into concrete during combined transport and chloride transport only.

Table 6. Composition of the concrete specimen.

Materials used (Saillio, 2013)	Value
Gravel 4/10 mm	1009 kg/m^3
Sand	905 kg/m^3
Cement CEM I	225 kg/m^3
Binder quantity	300 kg/m^3
Chemical admixture	6.5 kg/m^3
Water	159 kg/m^3
W/B	0.53

5. Experimental validation

Very few experimental data can be found on the coupled transport of chloride ions and carbon dioxide in unsaturated concrete. Saillio (2013) carried out a series of experiments to quantify the different phases of the cement matrix and its chloride binding by means of chloride binding isotherms for carbonated and non-carbonated cement based materials. To validate our model, we used these experimental data of Saillio (2013).

Various concretes were designed with the same clinker and aggregates with different percentages for metakaolin (10-25-30% MK). We choose for our simulation the concrete with 25% MK and 22% of water porosity. The composition and the properties of the concrete are listed in the Table 6 (Saillio, 2013).

The background of the experimental data of Saillio is presented as follows: The concrete specimen was subjected to a combined deterioration; 1 year of wetting by immersion in 0.5 M NaCl solution (chloride attack) and 2 months of exposure to air where the concentration of CO_2 was 1.5% by volume (carbonation in accelerated conditions). The relative humidity during the experiment was fixed to 65%.

Before performing a combined deterioration analysis, the coefficient of diffusion was determined from steady-state chloride migration test. The concrete specimen is subjected to a 30 V applied DC voltage. The upstream cell contains a 0.5 mol/L NaCl and 0.1 mol/L NaOH solution and the downstream cell a 0.1 mol/L NaOH solution. During the test chloride ions migrate from upstream to downstream due to the electrical field. The results provided the coefficient of diffusion $D_{Cl} = 1.5\times 10^{-12}$ m^2/s. The bound and free chlorides are adjusted with a Langmuir function as shown in Figure 9 .The other input parameters are directly calculated from the model equations introduced in Section 3.

In (Saillio, 2013), the concentration of the chloride ions has been measured with the respect to the depth in the specimen before and after carbonation. The chloride penetration depth has been measured by silver nitrate.

Figure 10 describes the simulated concentration profiles of free chlorides in both cases: combined deterioration (carbonation and chloride diffusion) and chloride transport only. These results are

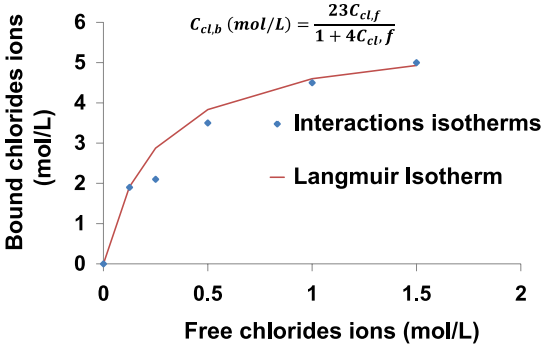

Figure 9. Binding isotherms.

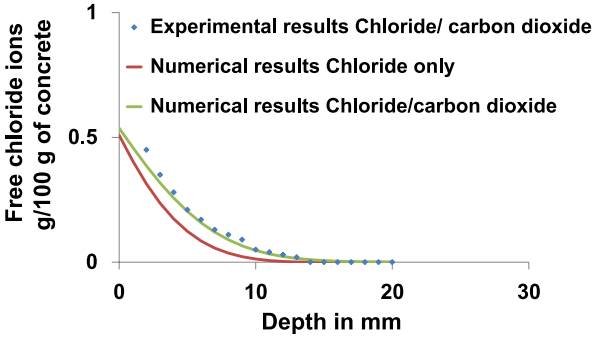

Figure 10. Chloride ions and carbon dioxide transport into concrete specimen: comparison between experimental and numerical results after one year of exposure to chloride ions and 2 months to carbon dioxide.

compared with those measured experimentally on the concrete specimen exposed to carbon dioxide and chloride ions.

Figure 10 clearly shows the influence of carbonation on free chloride concentration. The effect of carbon dioxide cannot be neglected. During the carbonation process, the bound chloride ions are released into the pore solution so that the concentration of free chloride ions increases. Consequently, the initiation time of reinforcement corrosion is significantly reduced by the combined mechanism.

Finally, the good agreement between the experimental results and the coupled simulation in Figure10 shows that the developed model is able to simulate combined diffusion of chloride and CO_2 in several conditions of exposure.

6. Conclusions

A numerical model has been proposed to simulate the combined carbonation and chloride ingress into concrete exposed to cyclic drying and wetting conditions. The ingress of ions by diffusion and convection is predicted taking into account electrostatic interactions and chemical activities of ions. The model is implemented in 1 D. The present study and analysis enable the following conclusions:

- The model allows to describe the penetration profiles of ions, the penetration depth of carbon dioxide and to predict the service life of concrete cover. Results show that CO_2 reacts with Friedel's salt, the latter increases the penetration depth of free chloride and decreases the penetration depth of carbon dioxide.

- The influence of carbonation on the microstructure properties is taken into account via the evolution of the porosity of concrete which decreases due to the production of calcite and silica gel.
- The rate of cyclic drying and wetting conditions influences the transport of chloride and other ions.
- The applicability and the validity of the model have been investigated by carrying out a comparison with Saillio's experimental study. The results indicate that the distribution of chlorides in concrete exposed to combined deterioration can be reasonably described by the developed model.

Acknowledgement

This work was carried out in the framwork of *MODEVIE* project. Support from the *Agence Nationale de la Recherche* (*ANR*) (National Research Agency, France) is gratefully acknowledged.

References

Ababneh, A., & Xi, Y. (2002). An experimental study on the effect of chloride penetration on moisture diffusion in concrete. *Materials and Structures, 35*(254), 659–663.

Amiri, O., & Aït-mokhtar, A. 2007. Presse de l'école nationale des ponts et chaussées. *GrandDubé «Rapport Synthétique SurLes Méthodes de Détermination Des Coefficients de Diffusion Apparent et Effectif »* [GrandDubé «Synthetic Report on Methods of Determination of Apparent and Effective Diffusion Coefficients].

Baroghel-bouny, V. 1994. *Caractérisation Microstructurale et Hydrique Des Pâtes de Ciment et Des Bétons Ordinaires et À Très Hautes Performances* (PhD thesis). Ecole nationale des ponts et chaussées.

Bel Japan, I. C. 2010. *Automatic Vapor Adsorption Measurement BELSORP-aqua3*. Specifications and features Catalog.

Buchwald, A. 2000. Determination of the ion diffusion coefficient in moisture and salt loaded masonry materials by impedance spectroscopy. In *3rd International Symposium Vienna* (pp. 475–482). Wien, Austria.

Debye, P., & Huckel, E. (1923). *Zur Theorie Der Elektrolyte*. Berlin Heidelberg: Springer. http://link.springer.com/10.1007/978-3-642-94260-0.

Despres, B. 2014. *Methodes Numeriques Pour Les EDP Instationnaires : Differences Finies et Volumes Finis*. Notes pour le cours de base M2-Mathematiques de la modelisation.

El Jouhari, N. 2011. *Cristallochimie Chimie Minérale*. University Mohammed 5 -AGDAL Faculty of Sciences.

van Genuchten, M. Th. (1980). A closed-form equation for predicting the hydraulic conductivity of unsaturated soils1. *Soil Science Society of America Journal, 44*(5), 892.

Khokhar, M. I. A., Rozière, E., Turcry, Ph., Gronfin, F., & Loukili, A. (2010). Mix design of concrete with high content of mineral additions: Optimisation to improve early age strength. *Cement and Concrete Composites,32*(5), 377–385.

Lee, C.-s., & Yoon, I.-S. (2003). Prediction of deterioration process for concrete considering combined deterioration of carbonation and chlorides ion. *Korea Concrete Institute, 15*, 902–912.

Leemann, A., & Moro, F. (2017). Carbonation of concrete: The role of CO_2 concentration, relative humidity and CO_2 buffer capacity. *Materials and Structures, 50*(1), 2–14.

LeVeque, R. (1998). Finite difference methods for differential equations. *Draft version for use in AMath*: 1998–2005. Retrieved from http://volunteerlecturerprogram.com/wp/wp-content/uploads/2013/01/lecnotes.pdf

Liu, R., Jiang, L., Xu, J., Xiong, C., & Song, Z. (2014). Influence of carbonation on chloride-induced reinforcement corrosion in simulated concrete pore solutions. *Construction and Building Materials, 56*, 16–20. doi:10.1016/j.conbuildmat.2014.01.030

Mai-Nhu, J. 2013. Corrosion Des Armatures Du Béton: Couplage Carbonatation/chlorures En Présence Des Cycles Hydriques (PhD thesis). Université de toulouse.

Marcus, Y. (2005). The standard partial molar volumes of ions in solution. *Journal of Molecular Liquids, 118*, 3–8.

Millington, R. J. (1959). Gas diffusion in porous media. *Science, 130*, 100–102.

Morandeau, A. (2013). Carbonatation Atmosphérique Des Systèmes Cimentaires À Faible Teneur En Portlandite (PhD thesis). Paris-Est.

Mualem, Y. (1976). A new model for predicting the hydraulic conductivity of unsaturated porous media. *Water Resources Research, 12*(3), 513–522. Retrieved from http://www.agu.org/pubs/crossref/1976/WR012i003p00513.shtml

Nguyen, P. T., & Amiri, O. (2016). Study of the chloride transport in unsaturated concrete: Highlighting of electrical double layer, temperature and hysteresis effects. *Construction and Building Materials, 122*, 284–293. doi:10.1016/j.conbuildmat.2016.05.154

Nguyen, T. Q. (2008). Physicochemical Modelling of Chloride Ingress into Cementitious Materials (PhD thesis). Ecole nationale des ponts et chaussées.

Pankow, J. F. (1994). *Aquatic chemistry concepts*. Boca Raton, FL: Lewis Publishers.

Papadakis, V. G., Vayenas, C. G., & Fardis, M. N. (1991). Physical and chemical characteristics affecting the durability of concrete. *ACI Materials Journal, 8*(88), 186–196. Retrieved from http://www.concrete.org/PUBS/JOURNALS/OLJDetails.asp?Home=MJ&ID=1993

Phu Tho, N. (2014). *Étude Multiphysique Du Transfert de Chlorures Dans Les Bétons Insaturés : Prédiction de L'initiation de La Corrosion Des Aciers* (PhD thesis). Université de la rochelle.

Ramezanianpour, A. A., Ghahari, S. A., & Esmaeili, M. (2014). Effect of combined carbonation and chloride ion ingress by an accelerated test method on microscopic and mechanical properties of concrete. *Construction and Building Materials, 58*, 138–146. doi:10.1016/j.conbuildmat.2014.01.102

Saeki, T. (2002, September). *Effect of carbonation on chloride penetration in concrete*. Third Rilem workshop on testing and modelling the chloride ingress into concrete, Madrid, Spain.

Saillio, M. (2013). *Bétons Sains Ou Carbonatés : Influence Sur Le Transport Ionique Spécialité : Structures et Matériaux Interactions Physiques et Chimiques Ions-Matrice Dans Les Bétons Sains et Carbonatés. Influence Sur Le Transport Ionique* (PhD thesis). Paris-EST-Marne-La-Vallée.

Samson, E., Marchand, J., & Beaudoin, J. J. (1999). Describing ion diffusion mechanisms in cement-based materials using the homogenization technique. *Cement and Concrete Research, 29*(8), 1341–1345.

Thiery, M., Dangla, P., Villain, G., & Platret, G. (2003). Modélisation Du Processus Physico - Chimique de Carbonatation Des Bétons. *Actes des Journées des Sciences de l'Ingénieur du réseau des LPC* (pp. 403–408). Dourdan, France.

Thiery, M. 2005. *Modélisation de La Carbonatation Atmosphérique Des Matériaux Cimentaires : Prise En Compte Des Effets Cinétiques et Des Modifications Microstructurales et Hydriques* (PhD thesis). Ecole nationale des ponts et chaussées. Retrieved from papers2://publication/uuid/F46A9B50-F797-4267-B6E6-FC248C0E9F75

Tumidajski, P. J., & Chan, G. W. (1996). Effect of sulfate and carbon dioxide on chloride diffusivity. *Cement and Concrete Research, 26*(4), 551–556.

Villain, G., & Thiery, M. (2006). Gammadensimetry: A method to determine drying and carbonation profiles in concrete. *NDT and E International, 39*(4), 328–337.

Wang, P., & Lu, W. (2007). Chloride penetration into integral water repellent concrete. *Restoration of Buildings and Monuments, 13*(1), 39–45.

Wang, X. (2012). *Modélisation Du Transport Multi-Espèces Dans Les Matériaux Cimentaires Saturés Ou Non Saturés et Éventuellement Carbonatés* (PhD thesis). Paris EST.

Wilke, C. R., & Chang, P. (1955). Correlation of diffusion coefficients in dilute solutions. *AIChE Journal, 1*(2), 264–270.

Xi, Y., Bažant, Z. P., & Jennings, H. M. (1994). Moisture diffusion in cementitious materials Adsorption isotherms. *Advanced Cement Based Materials, 1*(6), 248–257.

Zhang, M., Wang, P. G., & Wittmann, F. H. (2014). Influence of moisture content on chloride diffusion in concrete. *Restoration of Buildings and Monuments, 20*(2), 127–130.